PAPERS

Session 3

June 11th

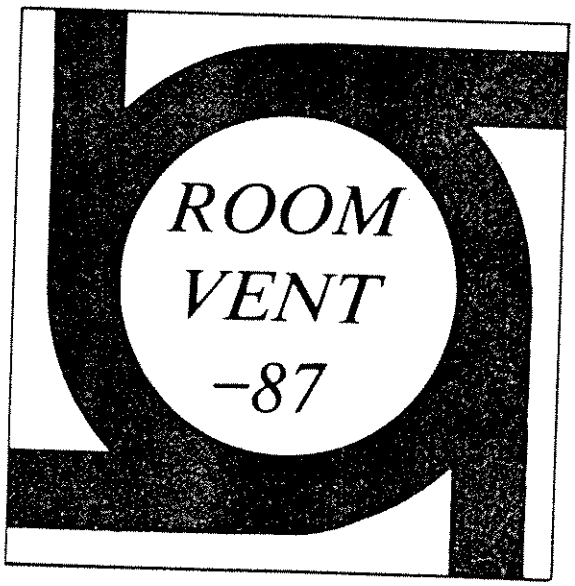

AIR DISTRIBUTION
IN
VENTILATED SPACES

Stockholm
Sweden
10—12 June 1987

A NUMERICAL INVESTIGATION OF THE LOCAL AGE AND THE LOCAL PURGING FLOW RATE IN TWO-DIMENSIONAL VENTILATED ROOMS

by

Lars Davidson* and Erik Olsson**

* Researcher

** Professor

Department of Applied Thermodynamics and Fluid Mechanics, Chalmers University of Technology, S-412 96 Gothenburg, Sweden

ABSTRACT

The buoyancy affected flows in three two-dimensional ventilated rooms are calculated; in two of the cases the predictions are compared with experimental data and the agreement is good.

The local age, τ_p, and the local purging flow rate, U_p, introduced by Sandberg and Sjöberg [1] are calculated for all cases. The former quantity is relatively easy to obtain experimentally, whereas there is, at the present time, no practical method for measuring the latter, which makes numerical investigation especially interesting. The number of stations at which the local age is obtained is considerably higher than anything done before experimentally, which means that a much more complete picture of the age field is obtained compared with earlier experimental investigations.

The local age attains high values and the local purging flow rate low values in stagnant regions, as expected. Sandberg and Sjöberg have theoretically formulated a relation between τ_p and U_p valid in regions of high age, which is confirmed. This relation restricts U_p more severely for higher values of τ_p and since there are regions of high age in the cases studied in this work (larger than twice the time constant of the system) confirmation of this relation is of some value.

NOMENCLATURE

c	concentration of contaminant
c_0	initial concentration
$C_{1\epsilon}$, $C_{2\epsilon}$, C_D, C_μ	constants in turbulence models
G	turbulence generating source term in the k- and ϵ-equations
g	acceleration due to gravity
H	height of room
h	height of inlet
k	turbulent kinetic energy
L	length of room
$\dot{m}$	mass flow rate
p	pressure
q_w	wall heat-flux per unit area
Q	total mass (volume) flow rate

t	time
T	temperature in ^oC
U, W	mean velocity in x and z-direction, respectively
U_i	mean velocity in x_i- direction
U^P	local purging flow rate
V	volume of the room
x, z	cartesian co-ordinates
x_i	cartesian co-ordinate in i-direction

Greek symbols

δ	length of a side of a quadratic control volume
Γ_ϕ	exchange coefficient of dependent variable
ϵ	dissipation of turbulent kinetic energy
μ, μ_{eff}, μ_t	dynamic viscosity (laminar, effective and turbulent, respectively)
ρ	density
σ_c, σ_k, σ_T, σ_ϵ	turbulent Prandtl number for concentration, turbulent kinetic energy, temperature and dissipation of turbulent kinetic energy, respectively
τ	age
τ_n	nominal time constant of system (room) (=V/Q)
ϕ	dependent variable

Subscripts

e	exit
in	inlet
P	arbitrary control volume
ref	reference value for the room
ϕ	dependent variable

1. INTRODUCTION

Two new ventilation parameters were (by Sandberg and Sjöberg [1], [2]) introduced a couple of years ago: the age and the local purging flow rate. The local age of the air at an arbitrary control volume within a room expresses how much time has elapsed, on an average, since the molecules entered the room. The local purging flow rate is the net rate (in [kg/s] or [m^3/s]) at which fluid (contaminant, for example) is 'flushed' out of the room from an arbitrary control volume P. Sandberg [3] has shown that knowledge of the local age provides useful information on how the air and the contaminants spread in ventilated rooms. As there does not yet exist an experimental method for measuring the local purging flow rate, numerical simulation of this parameter is especially interesting.

Above and in the following the term 'control volume' is used. For readers not familiar with numerical methods in fluid dynamics, it should be explained that the computation domain, i.e. the ventilated room, is divided into control volumes (i.e. vessels, compartments, boxes), which, in case of two-dimensional configurations, are of unit length in the third coordinate direction.

The authors have recently investigated the local age and the local purging flow rate [4]. The calculated local age field was compared with some experimentally obtained data [3], and the agreement between calculations and experiments was rather good. Sandberg and Sjöberg [1] have, theoretically, formulated a relation between the local age and the local purging flow rate

$$\tau_p U_p \leq V, \text{ when } \tau_p > \tau_n \qquad (1)$$

which is valid for regions where the age is high. This relation was confirmed by the authors for a two-dimensional isothermally ventilated room [4]. The validity of this relation is put to a more severe test in ventilation situations where regions of high age occur, because U_p in Eq. (1) is more restricted in these regions. The aim of the present study is, mainly, twofold:

i to calculate the local age and the local purging flow rate in ventilated rooms where regions of high age occur, in order to 'prove' or 'disprove' Eq. (1).

ii to enhance the physical understanding of the local age and the local purging flow rate by showing calculated fields of these two parameters for some ventilated rooms.

It was shown in [4] that stagnant regions (characterized by high local age and low purging flow rate) and well ventilated regions (low τ_p and high U_p) are readily identified from either the τ_p-field or the U_p-field. But as the local age is a transient parameter and the local purging flow rate is a steady one, knowledge of both parameters is necessary in order to fully characterize the performance of the system (ventilated room).

The computer program, the solution method and the boundary conditions are presented in the following section. There is a description in Section 3 of how the ventilation parameters are calculated. Results are presented and discussed in Section 4, and in the last section conclusions are drawn.

2. SOLUTION PROCEDURE

A computer program by Davidson and Hedberg [6], which is a derivative of TEACH-T by Gosman and Ideriah [7], has been used. This program solves equations of the type

$$\frac{\partial}{\partial t}(\rho\phi) + \frac{\partial}{\partial x_i}\left(\rho U_i \phi - \Gamma_\phi \frac{\partial \phi}{\partial x_i} \right) = S_\phi \qquad (2)$$

by expressing them in finite difference form. The finite difference equations are solved by a procedure which is based on the SIMPLE procedure introduced by Caretto et al [8] (see also e.g. Patankar [9]). The four main features are: staggered grids for the velocities; formulation of the difference equations in implicit, conservative form, using hybrid upwind/central differencing; rewriting of the continuity equation into an equation for the pressure correction; and iterative solving of the equations.

In the present calculations the dependent variable in Eq. (2) takes the forms: U, W, T, k, ϵ, c, τ_p, and 1 (continuity equation). The corresponding coefficients, Γ_ϕ, and sources, S_ϕ, are defined in Table 1.

Table 1. Definition of Γ_ϕ and S_ϕ for conservation equations solved

Equation	ϕ	Γ_ϕ	S_ϕ
Continuity	1	0	0
Momentum	U	μ_{eff}	$-\partial p/\partial x$
Momentum	W	μ_{eff}	$-\partial p/\partial z+\rho g \frac{T-T_{ref}}{T_{ref}+273}$
Temperature	T	μ_{eff}/σ_T	0
Turbulence energy	k	μ_{eff}/σ_k	$G - \rho\epsilon$
Turb. dissipation	ϵ	$\mu_{eff}/\sigma_\epsilon$	$\epsilon/k(C_{1\epsilon}G - C_{2\epsilon}\rho\epsilon)$
Concentration	c	μ_{eff}/σ_c	0
Local age	τ_p	μ_{eff}/σ_c	ρ

Notes:

1. $G \equiv \mu_{eff} \frac{\partial U_i}{\partial x_j} (\frac{\partial U_i}{\partial x_j} + \frac{\partial U_j}{\partial x_i})$; $\mu_{eff} = \mu + \mu_t = \mu + C_\mu \rho k^2/\epsilon$
2. Constants (see Launder and Spalding [11])
   $C_\mu = 0.09$; $C_{1\epsilon} = 1.44$; $C_{2\epsilon} = 1.92$; $\sigma_k = 1.0$; $\sigma_\epsilon = 1.3$
   $\sigma_T^\mu = 0.7$; $\sigma_c = 0.7$.

The Boussinesque approximation is used in the W-momentum equation to account for the density variations. The standard k-ϵ model [10] was used. No buoyancy sources were used in the turbulence model, since it was found that inclusion of these sources had little influence on the calculated flow pattern; furthermore inclusion of these sources slows down the convergence rate considerably.

Conventional wall functions [5], [10], were used when applying boundary conditions at the walls for U, W, T, k and ϵ. For c and τ_p zero flux (zero normal gradient) was imposed at the walls. Constant profiles at the inlet were set for all variables. At the outlet the exit velocity was calculated from mass balance, and zero streamwise gradient was imposed on the remaining variables.

3. VENTILATION PARAMETERS

Both the local age and the local purging flow rate are suitably calculated by using contaminants. In the present study dynamically passive contaminants have been used, i.e. the spreading of the contaminants does not influence the velocity field of the air. This means that the velocity field can be calculated first, and that the ventilation parameters can be calculated, using the calculated velocity field, introducing contaminants as appropriate.

The age of the air at a control volume within the room is the time that has elapsed since the air, passing this control volume, entered the room. In reference [4] the local age was calculated using the step-down method, i.e. the room was initially filled with contaminant, c_0, and the decay of the concentration was calculated. The local age was obtained from the formula

$$\tau_P = \frac{1}{c_0} \int_0^\infty c_p(t)\, dt \qquad (3)$$

A computationally much cheaper way of calculating the local age (which was also tested in [4]) is, as shown by Sandberg [2], to solve the (steady) transport equation (2) with $\phi = \tau_P$ and $S_\phi = \rho$, see Table 1. The boundary condition was $\tau_P = 0$ at the inlet.

The local purging flow rate was originally defined by Zwirin and Shinnar [12] as

$$U_P = \dot{m}_P / c_P = Q\, c_e / c_P \qquad (4a)$$

which was shown to have the physical meaning of the net rate at which a contaminant is 'flushed' out of the system from control volume P, or, equivalently, the net rate at which fresh air is supplied to control volume P. With the physical meaning of U_P kept in mind, Eq. (4a) is easily derived. An amount of contaminant, $\dot{m}_P$, is continuously generated at control volume P in the room. This ($\dot{m}_P$) must also, when steady state is reached, pass out through the outlet, where the concentration is c_e and the mass flow rate Q ($\dot{m}_P \ll Q$). U_P is the (imaginary) mass flow rate which 'convects' contaminant from control volume P (where the concentration is c_P) to the outlet, so that conservation of contaminant gives

$$\dot{m}_P = U_P c_P = Q\, c_e \qquad (4b)$$

which, indeed, is identical to Eq. (4a).

It was shown in [4] that the calculated U_P is dependent on the size of the control volumes. In the present study (as in [4]) the flow field is calculated using unequal spacing of grid lines, since the option of using denser spacing of grid lines where steep velocity gradients are expected, and vice versa, is desirable. When the U_P-fields were calculated, grids with all control volumes quadratic and of equal size were used; the sides of the control volumes were chosen to be $\delta = 0.1$. The velocity field for the latter grid was calculated from the former so as to satisfy continuity.

4. RESULTS

Two configurations of two-dimensional buoyantly ventilated rooms for which measurements of velocity and temperature fields exist have been chosen as test cases. The experimental investigations have been carried out by Åkesson [13] (herafter denoted by Case Å) and Hestad [14] (Case H). These cases were chosen because the flow is very stagnant in some regions (especially in Case Å), which makes verification, or refutation, of Eq. (1) more valuable (see Section 1). In order to accomplish a region of higher local age than in Case Å, a third configuration was chosen by modifying the wall boundary conditions for the temperature in Case Å [herafter denoted by Case ÅM (Åkesson Modified)]. The three configurations are shown in Fig. 1, geometrical data are summarized in Table 2, and boundary conditions are summarized in Table 3.

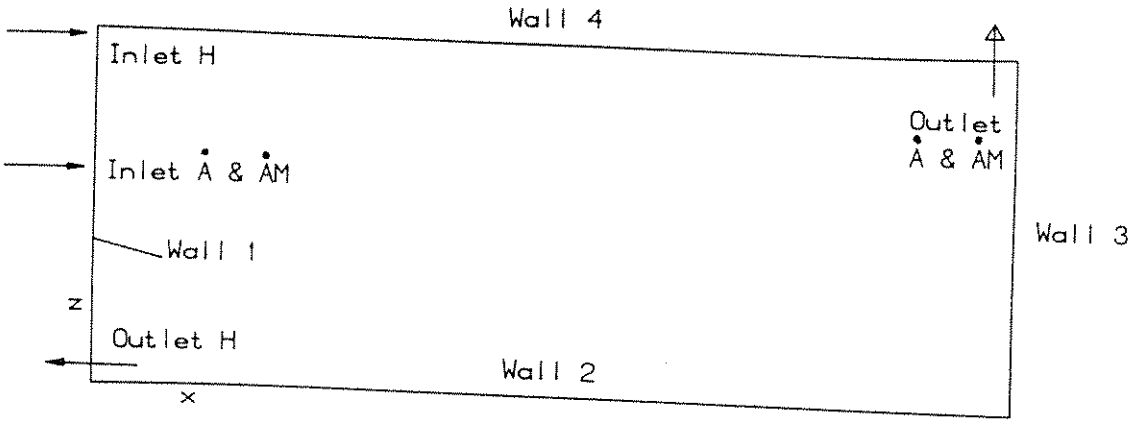

Figur 1. Configurations

Table 2. Geometrical data for the three configurations

Case	H [m]	L/H	h/H	y_{in}/H	τ_n [h]	Q [m^3/h]
Å,ÅM	2	2	0.003	0.6	0.12	65
H	2.82	2.56	0.007	1	0.19	106

The predicted and measured velocity vectors for Case Å are presented in Fig. 2, and the agreement between predictions and experiments is good. The predicted average temperature is 33°C, which should be compared with the experimental value of 25°C. Larsson [15], who also calculated the flow field for Case Å, reports also a predicted average temperature of 33°C. This discrepancy between predictions and experiments may be due to an inadequacy in the conventional wall-functions for predicting wall-heat flux. The authors [16] and Hanel and Scholz [17] have, however, accurately predicted the temperature field in a two-dimensional buoyantly ventilated room, where the

wall heat-flux was calculated by using conventional wall-functions. The reason for the discrepancy in temperature between predictions and experiments may, of course, also be due to a too low experimental value. A numerical grid with 29x23 nodes was used; a grid with 42x35 nodes was also tested and the results predicted with this grid differed very little from those predicted with the 29x23-node grid.

Table 3. Boundary conditions for the three configurations

Case	U_{in}	T_{in}	wall 1	wall 2	wall 3	wall 4
Å	3	55	T=13	q_w=0	q_w=0	T=15
ÅM	3	55	q_w=0	T=0	q_w=0	T=0
H	1.47	15	q_w=0	q_w=35.8	q_w=0	q_w=0

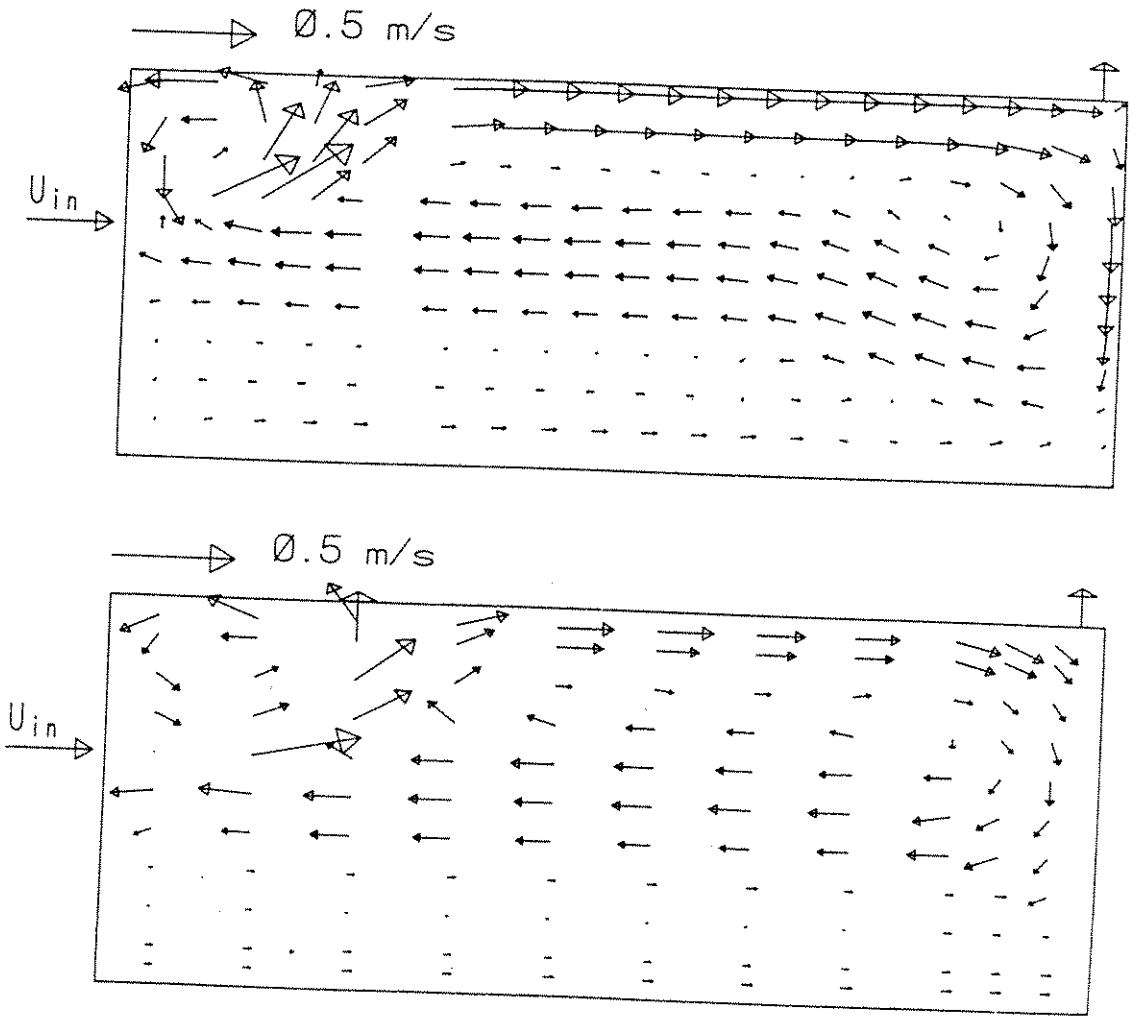

Figure 2. a) Calculated velocity vectors. b) Measured velocity vectors [13]. Case Å. Inlet and outlet velocities are not drawn to scale.

The predicted velocity vectors for Case H are shown in Fig. 3a. The point at which the wall jet separates from the ceiling is predicted as x=2.8 m, which agrees very well with the experimental value (=2.78 m). The predicted flow pattern with two large vortices, as well as the temperature field (predicted average temperature of 21.5°C) agree well with experiments (Hestad [14] reports an average temperature of 22°C). A numerical grid with 34x30 nodes was used. A grid with 51x39 nodes was also tested and the flow field predicted with this grid agrees well with that predicted with the 34x30-node grid.

The predicted velocity vectors for Case ÅM are shown in Fig. 4a. When this flow pattern is compared with that for Case Å in Fig. 2, it seems that the flow in the lower part is more stagnant than in Case Å, as intended. A 29x23-nodes grid (the same as for Case Å) was used.

The predicted local age and the local purging flow rate are shown in Figs. 3b, c (Case H), Figs. 4b, c (Case ÅM), and Fig. 5 (Case Å). For Case Å there is a large stagnant region in the lower part of the room ($\tau_p/\tau_n > 1.5$). When the boundary conditions for the temperature at the walls are altered (Case ÅM), the region near the corner below the outlet becomes very stagnant (τ_p/τ_n up to 3.6). The air in the right half of the room in Case H is, as expected, older than that in the left half. The predicted average age for the three cases were as follows: $\tau/\tau_n = 1.3$ for Cases Å and ÅM, and $\tau/\tau_n = 1.1$ for Case H.

The local purging flow rate attains, generally, low values where the age is high and vice versa. The exceptions are in the recirculating regions near the inlet (Cases Å and ÅM: above the inlet; Case H: below and right of the inlet). Here U_p is small because the amount of supplied fresh air is small (due to recirculation), whereas the air in this region is not very old. Regions where U_p is high [low c_p => high U_p, see Eq. (4)] are suitable for locating sources of contaminant, e.g. smoking persons, working stations for welding, etc. At the inlet and the outlet, for example, U_p attains its highest value (=Q); both places are comfortable for the smoker (provided $\dot{m}_p$ is the only source of contaminant), whereas the inlet is a very unsuitable location of the smoker from the point of view of the environment. It may be noted that the local purging flow rate field gives information only on how the smoker (the welder, etc.) experiences his/her ventilation situation when no other contaminant sources are present in the environment. The outlet, for example, may be a uncomfortable place to smoke at (although U_p=Q), since the air, when it eventually reaches the outlet, may be very contaminated. The question may arise how U_p can be large (=Q) at both the inlet and the outlet considering its physical meaning (i.e. the net rate at which contaminant is 'flushed' out of the system from P). The key word is net, which indicates that U_p denotes the fluid (contaminant) which leaves control volume P and does not return to P. So U_p is high at the inlet since no contaminant enters the control volume, i.e. no contaminant which leaves P ever returns to P.

The relation in Eq. (1) is confirmed for all three configurations. As is gathered from Eq. (1) the local purging flow rate is more restricted the higer values τ_p attains. In Fig. 6 the field of $\tau_p U_p/V$ for Case ÅM is shown. It is seen that although the local age increases nearer the lower right corner of the room (see Fig. 4b) $\tau_p U_p/V$ decreases, which means that U_p decreases faster than τ_p increases. It seems thus that Eq. (1) is satisfied by larger margin the larger τ_p is.

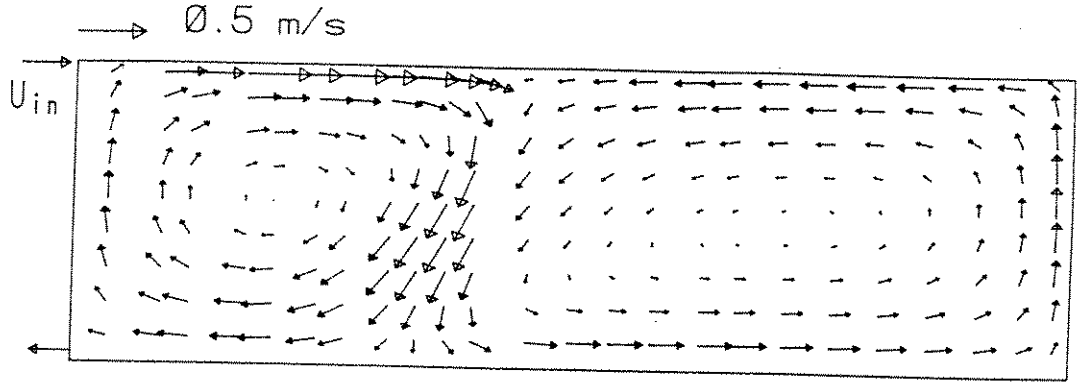

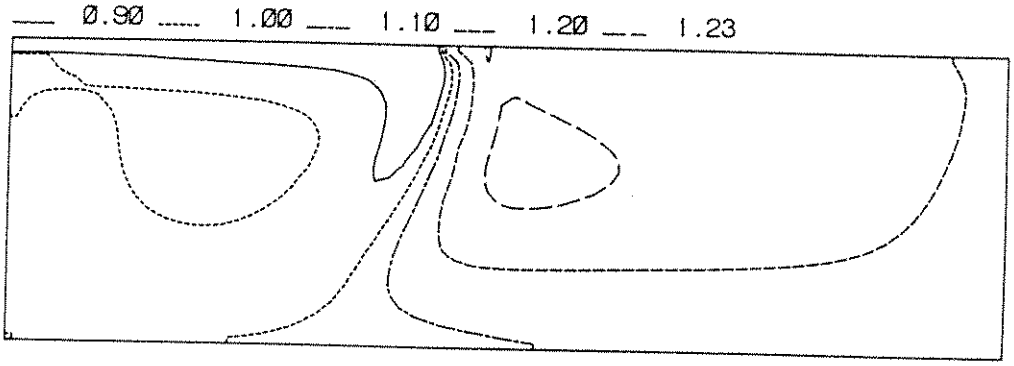

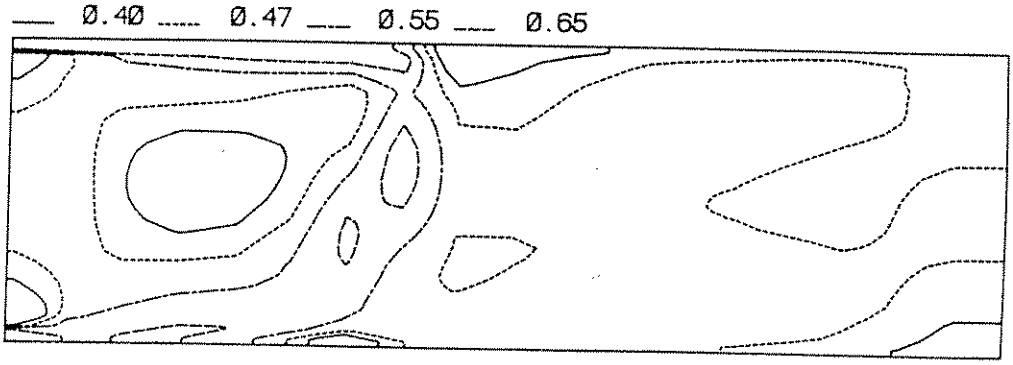

Figure 3. a) Calculated velocity vectors. Inlet and outlet velocities are not drawn to scale. b) Contours of calculcted local age scale with τ_n. c) Contours of calculated local purging flow rate scaled with Q. Case H.

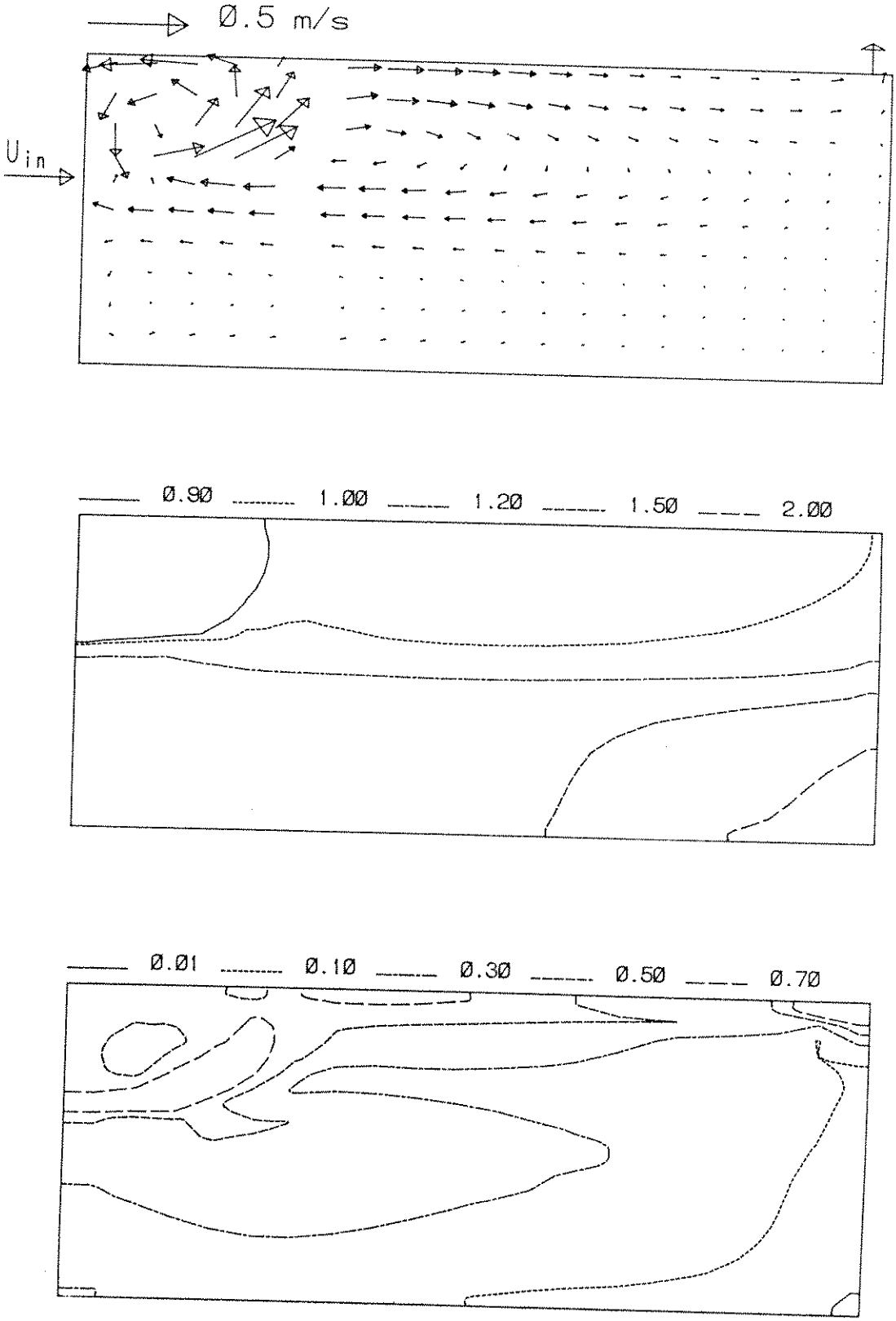

Figure 4. a) Calculated velocity vectors. Inlet and outlet velocities are not drawn to scale. b) Contours of calculated local age scaled with τ_n. c) Contours of calculated local purging flow rate scaled with Q. Case ÅM.

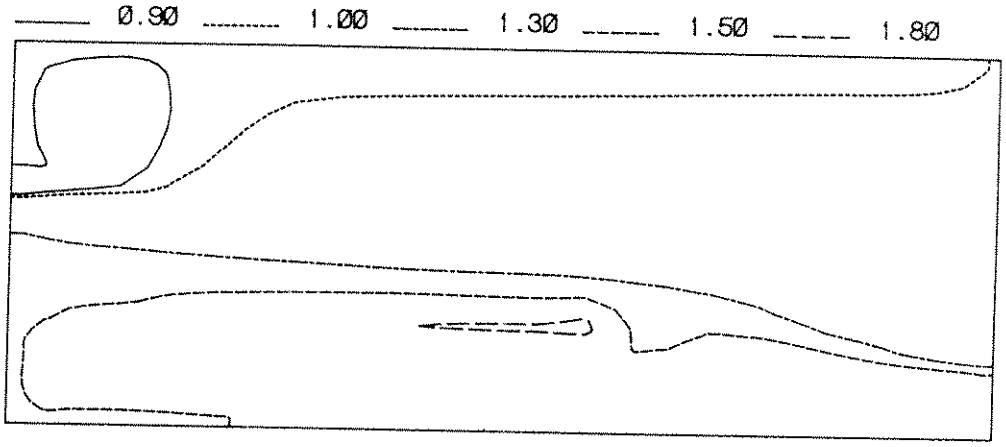

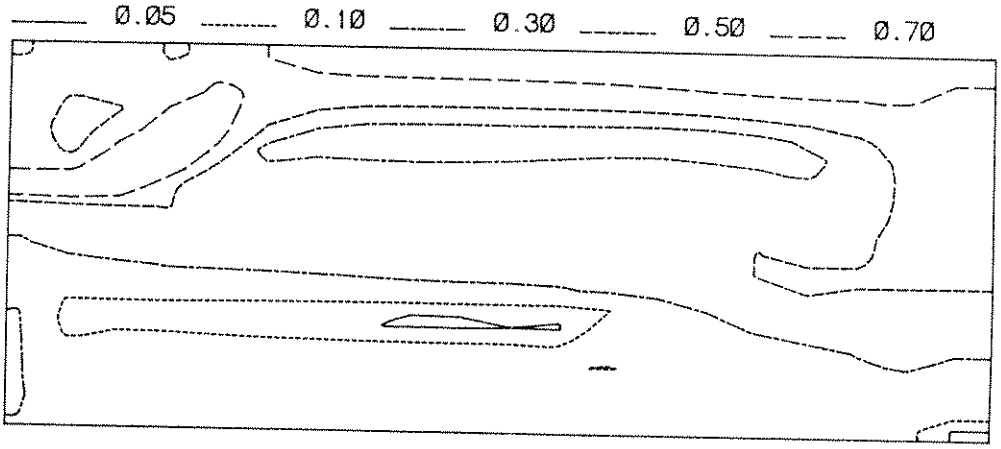

Figure 5. a) Contours of calculated local age scaled with τ_n. b) Contours of calculated local purging flow rate scaled with Q. Case Å.

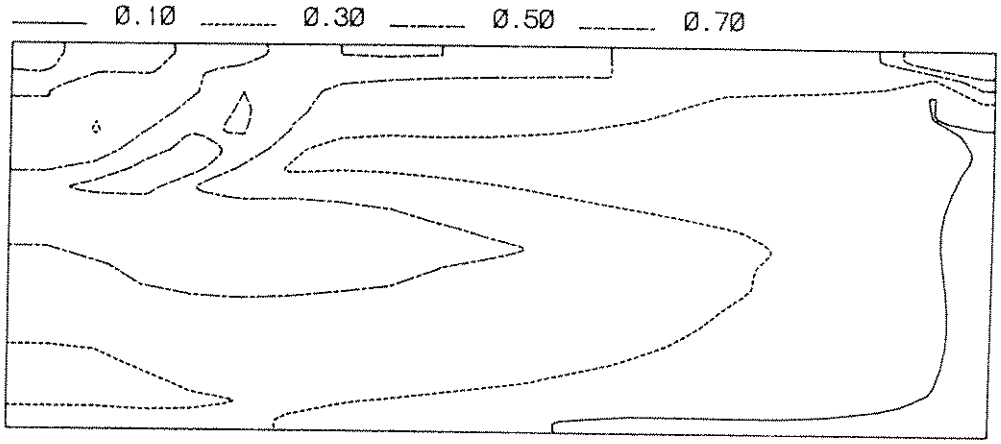

Figure 6. a) Contours of calculated $\tau_p U_p/V$ - field. Case ÅM.

It was mentioned in Section 3 that U_p is dependent on the size of the control volumes. The larger the control volume is, the larger U_p [4]. The question that may be put is: will Eq. (1) be satisfied for a grid with larger control volumes? In [4] the relation was confirmed using three different grids (δ=0.05, δ=0.1 and δ=0.2). A grid with δ=0.1 has been used above; when δ was increased to 0.2 Eq. (1) was still satisfied. To use even courser grids (e.g. δ=0.4) would not be meaningful for two reasons: first, U_p can not be considered to be a local quantity if too large control volumes are used, and, second, the velocity field can not be described accurately with too coarse a grid.

The required CPU-times on a VAX-750 machine are summarized in Table 4.

Table 4. Required CPU-time on a VAX-750 for different calculations

Case	flow-field [hours]	local age [min]	local purging flow rate [hours]
Å	2.1	0.25	2.0
ÅM	1*	0.25	2.0
H	1.0	0.9	14.0

*The results from Case Å were used as initial fields.

It can be seen that it is very expensive to calculate the U_p-fields. This is because a separate calculation has to be done for each control volume where U_p is to be obtained, by introducing a source of contaminant ($\dot{m}_p$) at P. Since the sides of the control volumes are δ=0.1, the grid, when calculating U_p, had the size 40x20 for Cases Å and ÅM, and 72x28 for Case H. U_p was calculated for every second control volume in the x-direction and for every one in the z-direction for Cases Å and ÅM; the corresponding figures for Case H were every fourth (x-direction) and every one (z-direction).

5. CONCLUSIONS

The velocity field has been calculated for three two-dimensional buoyantly ventilated rooms. For two of these configurations there exist experimental data, and the agreement between these and the calculations was good.

The local age and the local purging flow rate were calculated for all three configurations. The theoretically formulated relation between these parameters [Eq. (1)], formulated by Sandberg [1], was confirmed. This confirmation is considered to be of some value, since very stagnant regions occured for the configurations investigated in the present study; the local purging flow rate becomes more restricted according to Eq. (1) the more stagnant (=> high age) a region is. It was expected that the relation in Eq.

(1) would be satisfied by a smaller margin the higher values the local age attained; the opposite was shown to be the case.

ACKNOWLEDGEMENTS

The authors wish to thank Dr Mats Sandberg at the National Swedish Institute for Building Research who initiated the work on the ventilation parameters. The Swedish Council for Building Research has sponsored this work.

REFERENCES

1. Sandberg, M. and Sjöberg, M., "The Use of Moments for Assessing Air Quality", Bldg Environ., 18, 181-197 (1983).

2. Sandberg, M., "What Is Ventilation Efficiency?", Bldg Environ. 16, 123-135 (1981).

3. Sandberg, M., TM 279 (in Swedish), Dept. of Heating and Ventilation, Royal Institut of Tech., Stockholm (1984).

4. Davidson, L. and Olsson, E. , "Calculation of Age and Local Purging Flow Rate in Rooms", to be published in Bldg Environ. (1987) (se also [5]).

5. Davidson, L., "Turbulence Modelling and Calculation of Ventilation Parameters in Ventilated Rooms", thesis, Rept. 86/10, Dept. of Applied Thermodynamics and Fluid Mechanics, Chalmers Univ. of Tech., Göteborg (1986).

6. Davidson, L. and Hedberg, P., "A General Computer Program for Transient, Three-dimensional, Turbulent, Re-circulating Flows", Rept. 86/13, Dept. of Applied Thermodynamics and Fluid Mechanics, Chalmers Univ. of Tech., Göteborg (1986).

7. Gosman, A. D. and Ideriah, F. J. K., "TEACH-T: A General Computer Program for Two-dimensional, Turbulent, Recirculating flows", Dept. of Mechanical Engineering, Imperial College, London (1976).

8. Caretto, L. S., Gosman, A. D., Patankar, S. V., Spalding, D. B., "Two Calculation Procedures for Steady, Three-dimensional Flows with Recirculation", Proc. of the Third International Conference on Numerical Methods in Fluid Dynamics, 11, 60-68, publ. by Springer-Verlag Heidelberg, ed. by J. Ehlers, K. Hepp, H. A. Weidemuller (1972).

9. Patankar, S. V., "Numerical Heat Transfer and Fluid Flow", McGraw-Hill, New York (1980).

10. Rodi, W., "Turbulence Models and Their Application in Hydraulics", International Association of Hydraulic Research, Monograph, Delft, The Netherlands (1980).

11. Launder, B. E. and Spalding, D. B., "The Numerical Computation of Turbulent Flow", Comp. Meth. in Appl. Mech. and Eng., 3, 269-289 (1974).

12. Zvirin, Y. and Shinnar, R., "Interpretation of Internal Tracer Experiments and Local Sojourn Time Distributions", Int. J. Multiphase Flow, 2, 495-520 (1976).

13. Åkesson, K., "Experimentell bestämning av hastighets- och temperaturfördelningen i en ventilerad lokal" (in Swedish), Dept. of Applied Thermodynamics and Fluid Mechanics, Chalmers Univ. of Tech., Göteborg (1975).

14. Hestad, T., "Dimensjonering av innblåsningsventiler, kaldluft-nedfall" (in Norwegian), Norsk VVS, 6 (1976).

15. Larsson, M., "Predictions of Buoyancy Influenced Flow in Ventilated Industrial Halls", Proceedings of Heat Transfer in Buildings, Dubrovnik (1977).

16. Davidson, L. and Olsson, E. , "Calculation of Some Parabolic and Elliptic Flows Using a New One-equation Turbulence Model", to be presented at The 5th Int. Conf. on Numerical Methods in Laminar and Turbulent Flow, Montreal, (1987) (See also [5]).

17. Hanel, B. and Scholz, R., "Beitrag zur Modellierung zweidimensionaler isothermer und nichtisotermer turbulenten Strömungen in Räumen", Luft- und Kältetechnik, 15, 3-4 (1979).